AGU PUBLICATIONS

JGR

Journal of Geophysical Research: Space Physics

RESEARCH ARTICLE

10.1002/2015JA021427

Key Points:

- Unusual development of fresh and upward evolutionary-type EPBs near sunrise
- Fully depleted along flux tube and sustained for >90 mins of postsunrise hours
- Overshielding electric fields during a minor geomagnetic storm is responsible

Correspondence to:
S. Tulasi Ram,
tulasi@iigs.iigm.res.in

Citation:
Tulasi Ram, S., K. K. Ajith, M. Yamamoto, Y. Otsuka, T. Yokoyama, K. Niranjan, and S. Gurubaran (2015), Fresh and evolutionary-type field-aligned irregularities generated near sunrise terminator due to overshielding electric fields, *J. Geophys. Res. Space Physics*, *120*, 5922–5930, doi:10.1002/2015JA021427.

Received 5 MAY 2015
Accepted 23 JUN 2015
Accepted article online 25 JUN 2015
Published online 20 JUL 2015

Fresh and evolutionary-type field-aligned irregularities generated near sunrise terminator due to overshielding electric fields

S. Tulasi Ram[1,2], K. K. Ajith[1], M. Yamamoto[3], Y. Otsuka[4], T. Yokoyama[5], K. Niranjan[6], and S. Gurubaran[1]

[1]Indian Institute of Geomagnetism, Navi Mumbai, India, [2]On deputation to Solar-Terrestrial Environment Laboratory, Nagoya University, Nagoya, Japan, [3]Research Institute for Sustainable Humanosphere, Kyoto University, Kyoto, Japan, [4]Solar-Terrestrial Environment Laboratory, Nagoya University, Nagoya, Japan, [5]National Institute of Information and Communications Technology, Tokyo, Japan, [6]Department of Physics, Andhra University, Visakhapatnam, India

Abstract The unusual evolution of fresh and intense field-aligned irregularities (FAI) near sunrise terminator which further sustained for more than 90 min of postsunrise period was observed by Equatorial Atmosphere Radar at Kototabang during a minor geomagnetic storm period. These FAI echoes were initially observed around 250–350 km altitudes, growing upward under eastward polarization electric fields indicating the plasma bubbles that are fully depleted along the flux tube. The background low-latitude *F* layer dynamics that lead to the development of these dawn time FAI have been investigated from two ionosondes at near magnetic conjugate low-latitude locations. A minor geomagnetic storm was in progress which did not appear to cause any large electric field perturbations at preceding postsunset to midnight period over Indonesian sector. However, the prompt penetration of overshielding electric fields associated with sudden northward turning of interplanetary magnetic field B_z caused spectacular ascent of *F* layer and development of fresh, intense, and upward evolutionary plasma bubbles near sunrise terminator.

1. Introduction

The equatorial plasma bubbles (EPBs) and field-aligned irregularities (FAI) are one of the important space weather topics owing to their significant effects on satellite-based radio communications and navigational systems and have drawn continued interest because of its unpredictable variability on day-to-day and during geomagnetically active periods. The rapid uplift of equatorial *F* layer increases the growth rate of Rayleigh-Taylor (RT) instability by means of reduced ion-neutral collision frequency, hence one of the important prerequisites for the development of EPBs [*Fejer et al.*, 1999; *Tulasi Ram et al.*, 2006]. These local plasma-depleted (bubble like) structures induce at bottom side *F* region through RT instability and rapidly evolve to topside ionosphere via polarization electric fields within them [*Tsunoda et al.*, 2011; *Tulasi Ram et al.*, 2014]. The EPBs were essentially nighttime phenomena when the load conductivity at *E* region becomes minimal that liberates the polarization electric fields within the bubbles to grow. In the sunlit hemisphere, the refilling of plasma by photoionization and short circuiting of polarization electric fields by conducting *E* layer via highly conducting field lines make the conditions unfavorable for the growth and sustenance of EPBs.

The influence of geomagnetic storms on the generation or inhibition of EPBs is very complex and has been paid great attention during recent past owing to its important effects on satellite-based communication systems [e.g., *Basu et al.*, 2001; *Martinis et al.*, 2005; *Chakrabarty et al.*, 2006; *Tulasi Ram et al.*, 2008, 2015]. In general, the evolution or inhibition of EPBs during the geomagnetic storm periods will be controlled through the perturbations in the equatorial zonal electric field via two important processes, namely, prompt penetration electric fields (PPEFs) [*Nishida*, 1968; *Senior and Blanc*, 1984] and ionospheric disturbance dynamo [*Blanc and Richmond*, 1980]. The dynamic interactions between the solar wind and the Earth's magnetosphere that leads to sudden changes in the polar cap potential causing prompt penetration of interplanetary electric field (IEFy) to equatorial and low latitudes giving rise to transient perturbations in the zonal electric fields [*Senior and Blanc*, 1984; *Kikuchi et al.*, 2000; *Kelley et al.*, 2003; *Balan et al.*, 2012]. On the other hand, the ionospheric disturbance dynamo electric fields are due to global thermospheric wind circulation induced by Joule heating at high latitudes that generates long-lived (several hours) electric field perturbations at middle and low latitudes via ionospheric wind dynamo action

[*Blanc and Richmond*, 1980]. The local time dependence of the amplitude, phase, and polarity of induced electric fields due to these two processes, in fact, determines the development or inhibition of EPB irregularities at any given location [*Tulasi Ram et al.*, 2008; *Abdu,* 2011, and references therein]. For example, *Basu et al*. [2001, 2005] have shown the development of EPBs and abrupt onset of VHF/L-band scintillation due to prompt penetration of eastward IEFy in the dusk sector under southward orientation of interplanetary magnetic field (IMF) B_z. On the other hand, *Abdu et al.* [2009] and *Abdu* [2011] have reported a remarkable downward drift of equatorial *F* layer and inhibition of EPBs over Brazilian sector due to westward IEFy associated with northward turning of IMF B_z during postsunset hours. Using the Indian MST (mesosphere-stratosphere-troposphere) radar observations, *Chakrabarty et al*. [2006] have shown the initiation of EPBs due to eastward IEFy during postsunset hours, which were again resurrected into a plume-like structure around premidnight hours due to prompt penetration of overshielding electric fields. *Li et al.* [2012] have shown an interesting development of midlatitude irregularities over Japan around 1 h prior to the sunrise which were further extended to low latitudes and sustained longer under the influence of negative ionospheric storm due to ionosphere disturbance dynamo. Recently, *Santos et al.* [2012] have reported the increase of h_mF_2 and subsequent development of equatorial spread *F* during postmidnight hours over Fortaleza at 0050 LT and Jicamarca at 0130 LT due to disturbance dynamo electric field effects apparently modulated in a small degree by an overshielding eastward electric field. However, the evolution of fresh and intense EPBs near the sunrise terminator and their extended sustenance into postsunrise period is unexpected because of refilling by photoionization and increase in *E* region conductivity in the sunlit ionosphere. There were no such reports, except by *Fukao et al.* [2003a], on the evolution of fresh EPBs near sunrise terminator. *Fukao et al.* [2003a] have mentioned that the dawn time EPB event has occurred during the main phase of a storm, however, not investigated the responsible electric field perturbations. In this paper, an unusual development of three fresh and upward evolutionary plasma bubbles near sunrise terminator which further sustained for more than ~90 min of postsunrise period is reported from Equatorial Atmosphere Radar (EAR) observations in Indonesian sector during a minor geomagnetic storm on 27 February 2012. The corresponding changes in equatorial and low-latitude *F* layer dynamics which created favorable conditions for the development of these intense plume-like structures were studied in light of changes in IMF B_z and interplanetary electric fields.

2. Data and Observations

The Equatorial Atmosphere Radar (EAR) at Kototabang, Indonesia (0.2°S geographic latitude, 100.3°E geographic longitude, and 10.1°S dip latitude) operates at 47 MHz to study the *F* region field-aligned irregularities (FAI) at ~3 m scale size during nighttimes (18–06 LT). The detailed system specifications of EAR and its modes of operation have been reported by *Fukao et al.* [2003b] and *Yokoyama et al.* [2011]. The EAR is regularly operated at two sets of eight-beam (total 16 beams) *F* region mode that sequentially scans the beam directions on a pulse-to-pulse basis in order to obtain two-dimensional snapshots of backscatter echoes. The beam directions of these 16 beams are shown in Figure 1a. The fan sector backscatter maps constructed by combining the signal-to-noise ratio from these 16 beams provide a wide zonal (east-west) field of view (FoV) of ~500 km at 250 km altitude and ~800 km at 400 km altitudes and facilitate to observe the spatial and temporal evolution of EPBs over Indonesian region. The fresh and evolutionary-type EPBs can be identified (and can be distinguished from the fossil bubbles drifting from elsewhere) from these fan sector backscatter maps of EAR [e.g., *Ajith et al.*, 2015]. The EAR is also simultaneously operated in three sets of single-beam *F* region mode with azimuth angles fixed at 152.9° (eastward tilted beam), 180°(central beam, i.e., true south) and 207.1°(westward tilted beam) as shown in Figure 1b. This single-beam mode of observations can obtain the accurate Doppler velocity of FAI echoes within ± 398 m/s [*Yokoyama et al.,* 2011]. For *F* region observations, the zenith angles are chosen for all the radar beams to be perpendicular to the geomagnetic field line at 300 km altitudes. The background ionospheric conditions and the *F* layer dynamics are studied using two FM-CW (Frequency Modulated-Continuous Wave) ionosondes, one at Kototabang and another at northern magnetic low-latitude station, Chiang Mai (18.76°N geographic latitude, 98.93°E geographic longitude, and 12.7°N dip latitude). These FM-CW ionosondes at Kototabang (KTB) and Chiang Mai (CMU) were operated under South East Asia Low-latitude Ionospheric Network (SEALION). The Advanced Composition Explorer (ACE) satellite observations

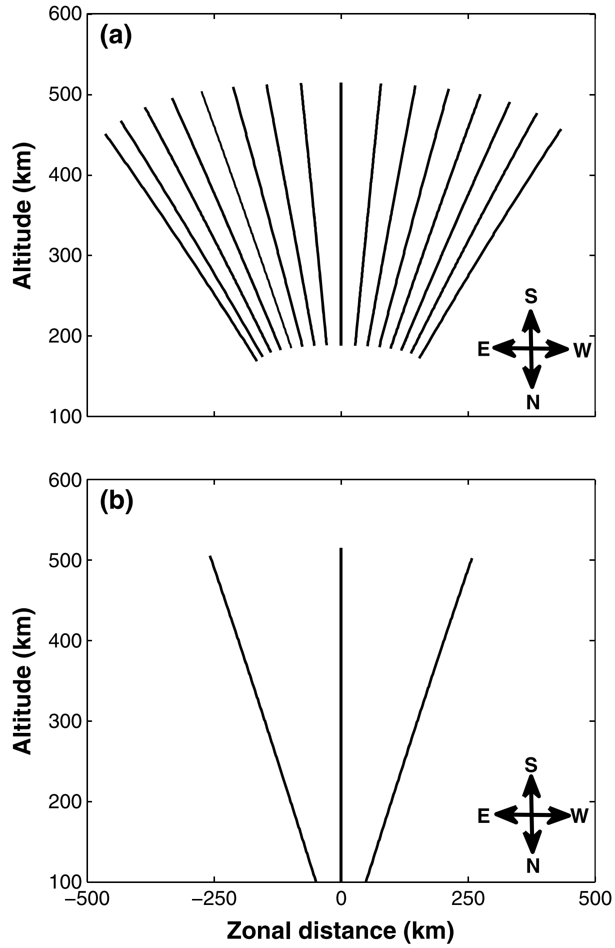

Figure 1. (a) The projections of multibeam (16 beams) *F* region mode observations in zonal distance and altitude plane used for constructing the fan sector backscatter maps. (b) The projections of three sets of fixed beam observations used for measuring the Doppler velocity of FAI echoes.

of interplanetary solar wind parameters considered in this study were time shifted to bow shock nose and obtained from space physics data facility at http://omniweb.gsfc.nasa.gov/ow_min.html. The geomagnetic storm index, *Dst*, is obtained from World Data Center for Geomagnetism of Kyoto University.

3. Results

The eruption of magnetic filaments on the Sun launched a coronal mass ejection (CME) around 0200 UT on 24 February 2012 which has hit the Earth's magnetosphere on 26 February at ~2200 UT. Figure 2 shows the time histories of interplanetary solar wind parameters observed from ACE satellite at first Lagrangian point (L1 point) and time shifted to bow shock nose along with the geomagnetic storm index, *Dst*. The sudden enhancement in solar wind velocity (Figure 2a) and density (Figure 2b) from their steady state values at 2200 UT on 26 February indicates the arrival of CME shock. The sudden compression of magnetosphere due to impingement of CME shock resulted in a sudden storm commencement (SSC) with *Dst* index sharply increasing to 20 nT at 2300 UT on 26 February. The IMF B_z turned to steady southward orientation around ~1200 UT on 27 February and the ring current enhancement caused the main phase onset (MPO) of a geomagnetic storm at 1300 UT. The IMF B_z remained steady southward for more than 7 h, however, caused only a minor geomagnetic storm with peak negative excursion of *Dst* reaching only −48 nT at 2000 UT. After remaining in steady southward state for several hours, the IMF B_z suddenly turned to northward around ~2000 UT triggering the recovery phase of the geomagnetic storm. This is in concurrent with the sudden decrease in solar wind density as can be observed from Figure 2b.

We now focus our investigation on the response of equatorial and low-latitude *F* layer for the changes in interplanetary electric field during this minor geomagnetic storm and its influence on the development of EPBs over Indonesian sector. Figure 3a shows the variation of dawn-to-dusk component of the interplanetary electric field (IEFy = $-V_{sw} \times$ IMF B_z) during 0900–2320 UT on 27 February 2012. The corresponding local time at Kototabang (~6 h 40 min ahead of UT) varies from 1540 to 0600 LT as shown in axis at top. Figure 3b shows the *F* layer base (virtual) height (*h*′*F*) variations from FM-CW ionosonde at two low-latitude stations, Kototabang (KTB) and Chiang Mai (CMU). The dotted lines with error bars represent the corresponding mean *h*′*F* variations of five international quiet days in February 2012 at KTB and CMU. The stations KTB and CMU are located on either side of geomagnetic equator at nearly magnetic conjugate locations [*Maruyama et al.*, 2007]. Unfortunately, we do not have the ionosonde observations at geomagnetic equatorial location during this period due to operational difficulties. However, from the simultaneous observations of *h*′*F* at magnetically conjugate locations of KTB and CMU, one can infer the perturbations in the equatorial zonal electric field in response to the

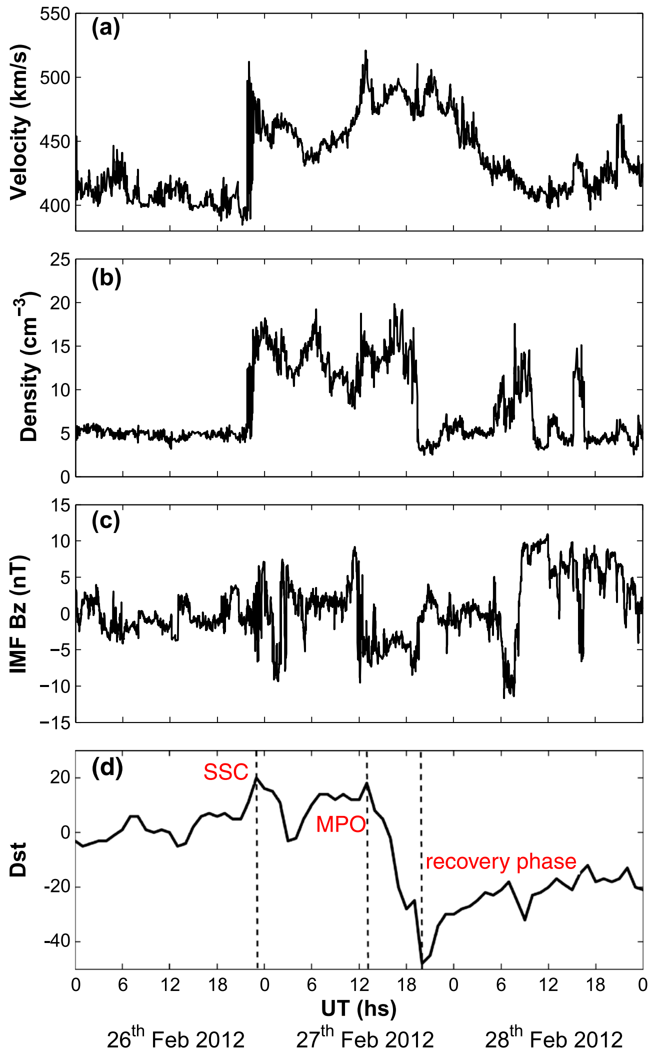

Figure 2. Time histories of (a) solar wind velocity (km/s), (b) solar wind density (cm^{-3}), (c) *Z* component of interplanetary magnetic field, IMF B_z (nT), and (d) geomagnetic storm index, *Dst*, during 26–28 February 2012.

changes in IEFy. In this study, the simultaneous upward drift of *F* layer (increase in *h′F*) at both the low-latitude, magnetically conjugate locations of KTB and CMU are attributed as mainly due to eastward electric field perturbation at the equator. Figure 3c shows the Altitude-Time-Intensity (ATI) map of equatorial plasma bubbles observed by EAR during this period. The red line shown in Figure 3c indicates the sunrise terminator at the corresponding apex altitude of field line over dip equator. A careful examination of the ATI map reveals that there are two intense EPBs during late postsunset hours (~2110 to 2210 LT or ~1430 to 1530 UT); and a small and weak EPB-like echo around local midnight (~2340 LT or ~1700 UT). Further, it is very interesting to observe the intense and upwelling plume-like structures around ~2126–2320 UT, i.e., near sunrise terminator and beyond.

The dawn-to-dusk component of interplanetary electric field (IEFy) is turned eastward at ~1200 UT. After a few initial fluctuations, the IEFy is more or less steadily eastward until ~1900 UT. This period corresponds to the local postsunset to midnight hours at Indonesian sector (1840 to 0140 LT). The *h′F* variation over KTB during the postsunset period is more or less similar to its quiet day mean variation, and the peak at 1300 UT is slightly smaller than its quiet day mean value. Further, the *h′F* at CMU also closely follows its quiet day mean variation during postsunset hours and does not exhibit any significant increase. The observed similarity in *h′F* variations with the corresponding quiet day mean variations at both KTB and CMU indicate that the effects of convection electric fields (eastward IEFy) at equatorial and low latitudes is negligible or minimal during this postsunset hours. Further, the observed variations of *h′F* over KTB and CMU are consistent with the quiet time variations of *h′F* during December solstice (December to February months) over Indonesian sector reported by *Maruyama et al.* [2007]. They have explained the uplift of *F* layer over KTB is predominantly due to northward transequatorial wind in addition to the smaller contribution from $E \times B$ drift due to prereversal enhancement of electric field (PRE) during postsunset hours. The steerable multibeam observations of EAR indicates (not shown in figure) that the two EPBs observed during 1430–1530 UT were not originated over KTB region, instead, drifted into FoV from some western longitudes. The *h′F* at both KTB and CMU again increases from 1530 UT and exhibits a small secondary peak at ~1700 UT (2340 LT). This simultaneous increase of *h′F* at both KTB and CMU around midnight is higher than their corresponding quiet day mean values. This elevated equatorial *F* layer during this period appears to cause favorable conditions for the initiation of a small plasma bubble around 1632 UT (2312 LT), however, that could not grow further and disappeared by 1650 UT

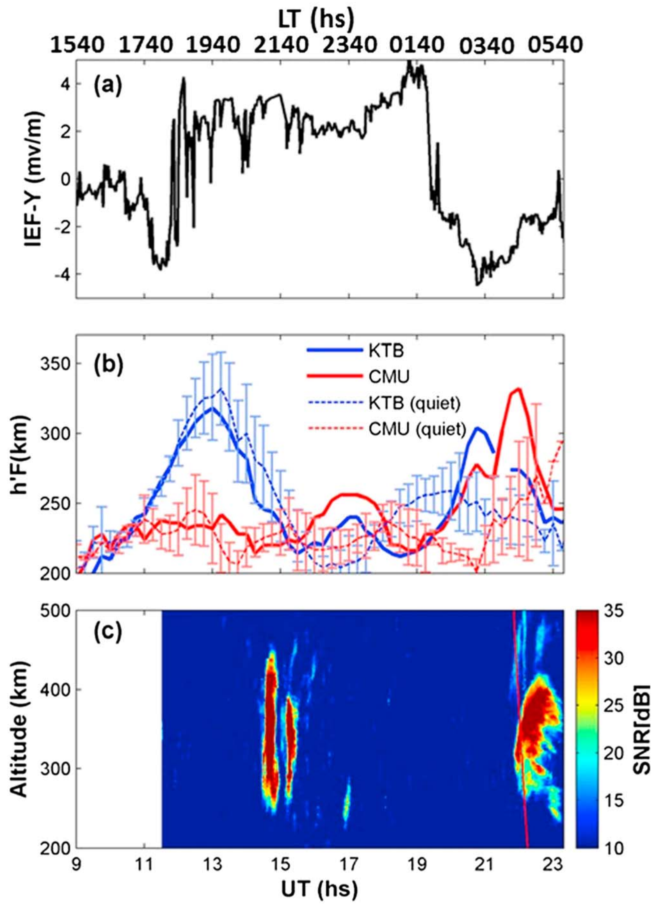

Figure 3. (a) Time variations of dawn-dusk interplanetary electric field, IEFy (mv/m), (b) *F* layer base (virtual) height (*h′F*) variations over Kototabang (KTB) and Chiang Mai (CMU) along with the corresponding five international quiet day mean variations (dotted lines with error bars), and (c) Altitude-Time-Intensity (ATI) map of *F* region field-aligned irregularities (FAI) observed by Equatorial Atmosphere Radar (EAR) during 0900–2320 UT on 27 February 2012. The red vertical curve indicates the sunrise terminator at apex altitude of field line over geomagnetic equator.

as can be seen from Figure 3c. The meager development and quick decay of this EPB is perhaps due to insufficient growth rate and quick descent of *F* layer at both KTB and CMU as can be observed from Figure 3b, probably due to the influence of geomagnetic storm.

The very interesting observation from Figure 3c is the unusual development of very intense (>35 dB) and upwelling plume-like echoes from 2126 UT, i.e., around the sunrise terminator, which are further found to be growing upward. These FAI echoes are continued to observe for more than 90 min after the *F* region apex sunrise, and the observations are stopped at 2320 UT due to regular schedule of EAR. Figure 4 shows the spatial and temporal evolution of these dawn time EPBs from the fan sector backscatter maps constructed from steerable multibeam (16 beams) observations of EAR during 2126–2320 UT. A faint FAI echo can be observed around 250–300 km altitude at 2126 UT indicated as EPB-1 in Figure 4. As the time progresses, this echo is successively growing within the FoV of EAR and developed into an intense EPB. At 2138 UT, another faint echo can be observed at the eastern edge of FoV around 280–330 km altitude (indicated as EPB-2) which is also successively growing and developed into an intense EPB by 2214 UT. Another FAI echo (EPB-3) can be observed around 400–450 km altitude at the western edge of FoV at 2147 UT. This echo (EPB-3) also successively growing with eastward expansion and fully developed into an intense EPB by 2247 UT. The EPB-2 and EPB-3 were progressively rising to higher altitudes and top altitudes of these EPBs exceeded 500 km (maximum detectable altitude from EAR) which corresponds to an apex altitude of ~712 km. The notable feature of these three EPBs is that they were not fossil bubbles drifted from elsewhere. Instead, all the three EPBs in Figure 4 were freshly initiated within or adjacent to the FoV of EAR, successively evolved into intense EPBs, and exhibit gradual decay without significant zonal drift. Further, these EPBs were continued to evolve and sustained for more than ~90 min of postsunrise period. While the EPB-1 is almost disappeared by 2320 UT, the other two EPBs (2 and 3) were sustained even at 2320 UT with less intensity.

With a view to further examine the Doppler velocities of these dawn time EPB echoes, the single-beam *F* region Doppler mode observations of EAR are considered. The beam directions fixed for three sets of single-beam Doppler mode observations are shown in Figures 1b and 4 at 2226 UT. As the EPBs shown in Figure 4 did not exhibit significant zonal drifts, the central beam (azimuth = 180°) is only observing the EPB-1 throughout the observation period. The eastern beam (azimuth = 152.9°) is mostly illuminating EPB-2 and a small portion of EPB-1. For example, Figures 5a and 5b show the ATV

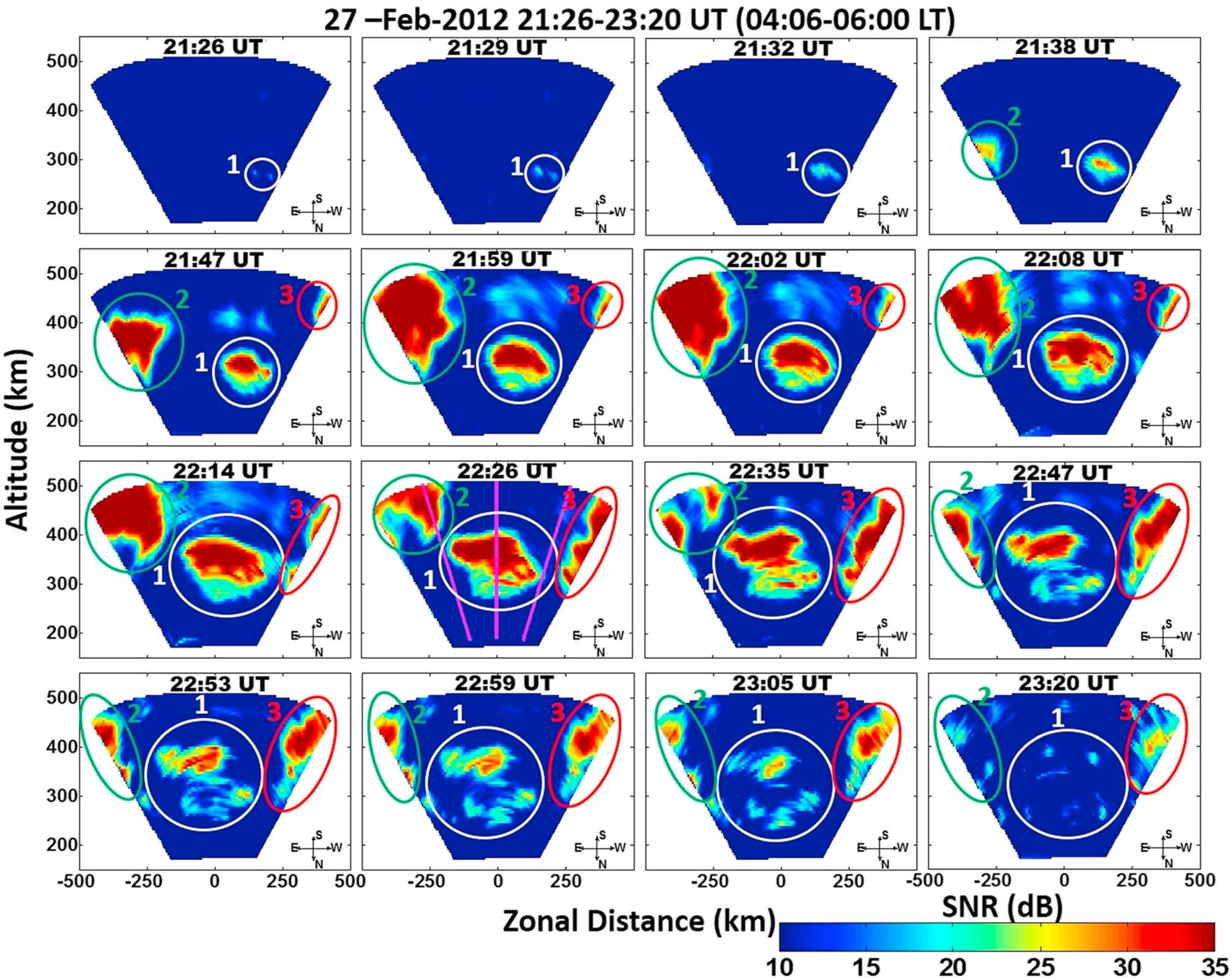

Figure 4. A series of fan sector backscatter echo maps showing the onset, evolution, and decay of three fresh EPBs over Indonesian sector during the local predawn hours (2126–2320 UT on 27 February 2012). The pink lines in fact sector map at 22:26 UT indicates the beam directions of three single-beam *F* region Doppler mode of operation (see Figure 1b and related text).

(altitude-time Doppler velocity) maps of these dawn time EPBs (EPB-1 and EPB-2) from the central and eastern beams, respectively. The western (azimuth = 207.1°) beam is also observing EPB-1 and mostly directed at the lower part of EPB-1, hence not shown. The red lines in Figure 5 represent the sunrise terminator at apex altitude of field line over dip equator, whereas the green lines represent the sunrise terminator at radar illuminating location. It is very interesting to observe from these figures that the EPB-1 and EPB-2 echoes exhibit dominant negative Doppler (upward drift) velocities near sunrise terminator and later. Though the Doppler velocity of EPB-1 (Figure 5a) is downward at altitudes below 350 km after 2230 UT, it continued to exhibit upward drift at higher altitudes up to ~2250 UT. The Doppler velocity of EPB-2 echo is predominantly upward (~50 m/s) at higher altitudes indicating that the upward evolution of EPB-2 is continued for more than 1 h after the sunrise (Figure 5b). The dominant negative Doppler (upward drift) velocities exhibited by these echoes further confirm that these EPBs are freshly generated around sunrise terminator and continued to evolve upward even during the postsunrise hours. The extended sustenance of these EPBs during the postsunrise period suggests that these EPBs are fully depleted along the flux tube, hence takes longer time to be refilled by photoionization. Further, the negative Doppler velocities indicate that the polarization electric fields within the EPBs are eastward that supported the extended growth and sustenance of EPBs during postsunrise period.

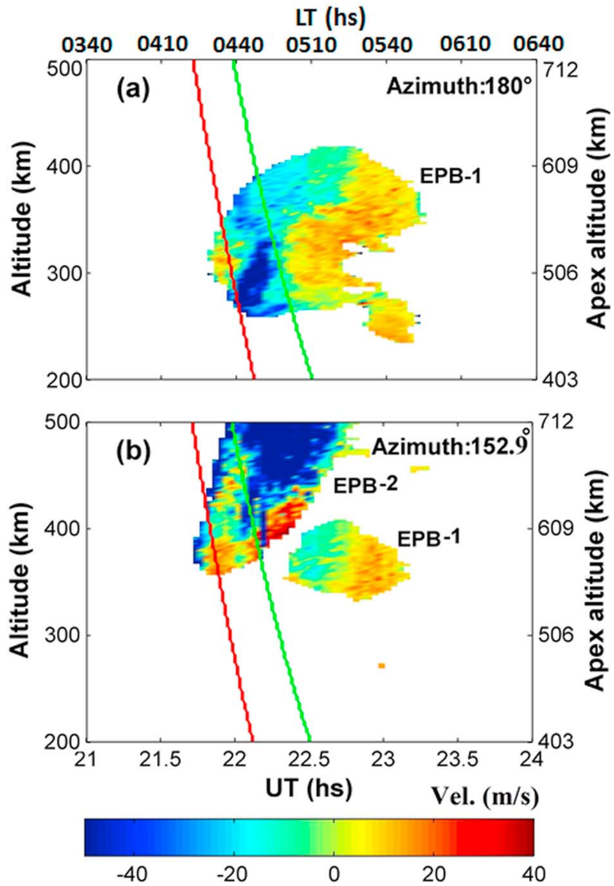

Figure 5. The ATV (altitude-time-Doppler velocity) maps of the freshly evolved dawn time EPB plumes observed by EAR. (a) Central beam (azimuth = 180°) observing EPB-1. (b) From eastward titled beam (azimuth = 152.9°) that is mostly illuminating EPB-2 and a small portion of EPB-1. The red vertical curves indicate the sunrise terminator at apex altitude of field line over geomagnetic equator, and the green vertical curves represent the sunrise terminator at radar illuminating location.

4. Discussion

The dynamic reconnection between the solar wind and Earth's magnetosphere during geomagnetic storm periods causes the convection of solar wind energy and enhanced field-aligned currents in region-1 and region-2 ionosphere (R1 and R2 FACs). During the main phase of the geomagnetic storms (under steady southward IMF B_z periods), the convection electric fields due to R1-FAC are often stronger than the shielding electric fields. This imbalance situation is called "undershielding" that allows penetration of IEFy and causes enhanced eastward electric field perturbations in day to postsunset sector [*Nishida*, 1968; *Kikuchi et al.*, 1996, 2000]. However, during the main phase of this storm around 1300 UT, the *h′F* at KTB and CMU did not show any significant enhancement compared to their mean quiet day variations under the southward IMF B_z (eastward IEFY) during postsunset hours (Figure 3b). This indicates that the effects of convection electric fields (eastward IEFy) at equatorial and low latitudes were minimal or negligible at the postsunset period over Indonesian sector during this minor geomagnetic storm. On the other hand, when the interplanetary magnetic field (IMF B_z) turns suddenly northward after a steady southward configuration, the R2-FAC can be momentarily stronger than the R1-FAC. This condition is known as "overshielding," and the dominant shielding electric fields penetrates to low latitudes causing eastward (westward) electric field perturbations in equatorial ionosphere at night to dawn (day to postsunset) sector [*Rastogi and Patel*, 1975; *Reddy et al.*, 1979; *Kelley et al.*, 1979, 2003]. It can be clearly observed from Figure 3b that the *h′F* at both KTB and CMU exhibits a spectacular ascent starting from ~1900 UT, concurrently with the sudden reversal of IEFy (Figure 3a) associated with the northward turning of IMF B_z (Figure 2c). This large uplift of *F* layer at both KTB and CMU indicates that the effects of overshielding electric fields are significantly large. This could be, probably, due to long-duration southward IMF B_z (more than 7 h) phase preceding its northward turning, which facilitates the large accumulation of shielding charges in the inner magnetosphere. When the IMF B_z turns suddenly northward, these shielding charges will temporarily out of balance and cause enhanced eastward electric field perturbations in the midnight-dawn sector. *Huang et al.* [2010] have shown that the ionospheric response to sudden northward turning of IMF B_z is significant after a long southward IMF B_z phase. The *h′F* at KTB increases continuously and reaches to a maximum of ~310 km at ~2045 UT which is remarkably higher than their quiet day mean values. The *h′F* at CMU also exhibits a simultaneous increase and reaches a maximum of ~340 km at ~2130 UT. Subsequently, the onset of three dawn time EPBs occurred at the time of peak upward excursion of *h′F* at KTB and CMU as marked in Figure 3b. This rapid ascent of *F* layer at both magnetically conjugate low-latitude locations, concurrently, with the sudden northward turning of IMF B_z gives the most convincing evidence for suddenly enhanced eastward electric perturbation due to overshielding

[*Rastogi and Patel*, 1975; *Kelley et al.*, 1979; *Fejer et al.*, 1979]. As a result, the equatorial *F* layer is elevated to much higher altitudes and created conditions conducive (sufficient growth rate for RT instability is achieved) for the evolution of fresh and intense EPBs. It should be mentioned that the onset of EPBs takes place around *F* region altitudes at geomagnetic equator, hence takes small but finite time to rise and map along the field lines to be detected by EAR at low latitude (10.1°S dip latitude). Considering this limitation of EAR and lack of observations over the equatorial location, the actual onset times of EPBs over equator would be a few minutes earlier than shown in Figures 3–5. Nevertheless, the simultaneous and rapid ascent of *h′F* at both KTB and CMU and subsequent development of EPBs clearly indicates penetration of overshielding electric field associated with sudden northward turning of IMF B_z is the main responsible factor for the development of fresh, intense, and evolutionary-type EPBs near sunrise terminator over Indonesian sector.

Further, these dawn time EPBs (EPBs 2 and 3) have progressively rising to topside ionosphere and the top altitudes of EPBs exceeded 500 km over KTB (~712 km at apex). The negative Doppler velocities of ~50 m/s indicate strong eastward polarization electric fields within bubbles that supported the extended growth of EPBs to higher altitudes. Further, the observed EPBs near sunrise terminator were sustained for more than 90 min of postsunrise period which indicates that these EPBs were fully depleted along the flux tube. Also, the photoionizaton after sunrise mostly takes place around *F* region altitudes (below 300 km); hence, it takes longer time for the fully depleted plasma bubbles at topside altitudes to be refilled by the photoionization.

5. Conclusions

An unusual and interesting development of fresh and intense EPBs near sunrise terminator was observed by Equatorial Atmosphere Radar over Indonesian sector which is further found to be growing upward even after the apex sunrise. A minor geomagnetic storm (*Dst* minimum of −48 nT) has occurred at preceding hours which did not appear to cause any large zonal electric field perturbations at preceding postsunset to midnight period over Indonesian sector. However, the sudden northward turning of IMF B_z resulted in prompt penetration of overshielding electric fields that elevated the equatorial *F* layer to much higher altitudes and created conditions conducive for the development of fresh, intense, and upward evolutionary EPBs near the sunrise terminator. The eastward polarization electric fields within the EPBs supported the extended growth and development of fully depleted EPBs which sustained for more than ~90 min of postsunrise period. These results importantly demonstrate that the fresh EPBs can evolve even at sunrise terminator when the equatorial *F* layer is sufficiently elevated (sufficient growth rate is achieved) and can sustain longer into postsunrise period under eastward polarization electric fields within the bubbles. Further, this study also exemplify the potential role of prompt penetration of overshielding electric fields on the development of EPBs even during a minor geomagnetic storm that can have important implications on transionospheric radio communication links.

Acknowledgments
This work is supported by DST, Government of India through project GITA/DST/TWN/P-47/2013 and partially supported by STEL international joint research program 2015. The EAR is operated by RISH, Kyoto University, Japan, and LAPAN, Indonesia (http://www2.rish.kyoto-u.ac.jp/ear/). This work was partly supported by JSPS KAKENHI grants 22403011 and 25302007, and MEXT Strategic Funds for the Promotion of Science and Technology. The authors thank NICT, Japan for providing ionosonde data of KTB and CMU through SEALION network (http://seg-web.nict.go.jp/sealion/). The authors acknowledge the open data policy of *Dst* index through WDC, Kyoto University, Japan (http://wdc.kugi.kyoto-u.ac.jp/) and ACE solar wind parameters through SPDF, NASA, USA (http://omniweb.gsfc.nasa.gov/ow_min.html).

Alan Rodger thanks two anonymous reviewers for their assistance in evaluating this paper.

References

Abdu, M. A. (2011), Equatorial spread F/plasma bubble irregularities under storm time disturbance electric fields, *J. Atmos. Sol. Terr. Phys.*, *75–76*, 44–56.

Abdu, M. A., E. A. Kherani, I. S. Batista, and J. H. A. Sobral (2009), Equatorial evening prereversal vertical drift and spread F suppression by disturbance penetration electric fields, *Geophys. Res. Lett.*, *36*, L19103, doi:10.1029/2009GL039919.

Ajith, K. K., S. Tulasi Ram, M. Yamamoto, T. Yokoyama, V. S. Gowtam, Y. Otsuka, T. Tsugawa, and K. Niranjan (2015), Explicit characteristics of evolutionary-type plasma bubbles observed from Equatorial Atmosphere Radar during the low to moderate solar activity years 2010–2012, *J. Geophys. Res. Space Physics*, *120*, 1371–1382, doi:10.1002/2014JA020878.

Balan, N., J. Y. Liu, Y. Otsuka, S. Tulasi Ram, and H. Lühr (2012), Ionospheric and thermospheric storms at equatorial latitudes observed by CHAMP, ROCSAT, and DMSP, *J. Geophys. Res.*, *117*, A01313, doi:10.1029/2011JA016903.

Basu, S., S. Basu, K. M. Groves, H. C. Yeh, S. Y. Su, F. J. Rich, P. J. Sultan, and M. J. Keskinen (2001), Response of the equatorial ionosphere in the South Atlantic region to the great magnetic storm of July 15, 2000, *Geophys. Res. Lett.*, *28*, 3577–3580, doi:10.1029/2001GL013259.

Basu, S., S. Basu, K. M. Groves, E. MacKenzie, M. J. Keskinen, and F. J. Rich (2005), Near-simultaneous plasma structuring in the midlatitude and equatorial ionosphere during magnetic superstorms, *Geophys. Res. Lett.*, *32*, L12S05, doi:10.1029/2004GL021678.

Blanc, M., and A. D. Richmond (1980), The ionospheric disturbance dynamo, *J. Geophys. Res.*, *85*, 1669–1688, doi:10.1029/JA085iA04p01669.

Chakrabarty, D., R. Sekar, R. Narayanan, A. K. Patra, and C. V. Devasia (2006), Effects of interplanetary electric field in the development of an equatorial spread F event, *J. Geophys. Res.*, *111*, A12316, doi:10.1029/2006JA011884.

Fejer, B. G., C. A. Gonzales, D. T. Farley, M. C. Kelley, and R. F. Woodman (1979), Equatorial electric fields during magnetically disturbed conditions: 1. The effect of the interplanetary magnetic field, *J. Geophys. Res.*, *84*, 5797–5802, doi:10.1029/JA084iA10p05797.

Fejer, B. G., L. Scherliess, and E. R. de Paula (1999), Effects of the vertical plasma drift velocity on the generation and evolution of equatorial spread F, *J. Geophys. Res.*, *104*, 19,859–19,869, doi:10.1029/1999JA900271.

Fukao, S., H. Hashiguchi, M. Yamamoto, T. Tsuda, T. Nakamura, M. K. Yamamoto, T. Sato, M. Hagio, and Y. Yabugaki (2003a), Equatorial Atmosphere Radar (EAR): System description and first results, *Radio Sci.*, *38*(3), 1053, doi:10.1029/2002RS002767.

Fukao, S., Y. Ozawa, M. Yamamoto, and R. T. Tsunoda (2003b), Altitude-extended equatorial spread F observed near sunrise terminator over Indonesia, *Geophys. Res. Lett.*, *30*(22), 2137, doi:10.1029/2003GL018383.

Huang, C.-S., F. J. Rich, and W. J. Burke (2010), Storm time electric fields in the equatorial ionosphere observed near the dusk meridian, *J. Geophys. Res.*, *115*, A08313, doi:10.1029/2009JA015150.

Kelley, M. C., B. Fejer, and C. Gonzales (1979), An explanation for anomalous equatorial ionospheric electric fields associated with a northward turning of the interplanetary magnetic field, *Geophys. Res. Lett.*, *6*, 301–304, doi:10.1029/GL006i004p00301.

Kelley, M. C., J. J. Makela, J. L. Chau, and M. J. Nicolls (2003), Penetration of the solar wind electric field into the magnetosphere/ionosphere system, *Geophys. Res. Lett.*, *30*(4), 1158, doi:10.1029/2002GL016321.

Kikuchi, T., H. Luhr, T. Kitamura, O. Saka, and K. Schlegel (1996), Direct penetration of the polar electric fields to the equator during a DP 2 event as detected by the auroral and equatorial magnetometer chains and the EISCAT radar, *J. Geophys. Res.*, *101*, 17,161–17,173, doi:10.1029/96JA01299.

Kikuchi, T., H. Luhr, K. Schlegel, H. Tachihara, M. Shinohara, and T. L. Kitamura (2000), Penetration of auroral electric fields to the equator during a substorm, *J. Geophys. Res.*, *105*, 23,251–23,252, doi:10.1029/2000JA900016.

Li, J., G. Ma, T. Maruyama, and Z. Li (2012), Mid-latitude ionospheric irregularities persisting into late morning during the magnetic storm on 19 March 2001, *J. Geophys. Res.*, *117*, A08304, doi:10.1029/2012JA017626.

Martinis, C. R., M. J. Mendillo, and J. Aarons (2005), Toward a synthesis of equatorial spread F onset and suppression during geomagnetic storms, *J. Geophys. Res.*, *110*, A07306, doi:10.1029/2003JA010362.

Maruyama, T., M. Kawamura, S. Saito, K. Nozaki, H. Kato, N. Hemmakorn, T. Boonchuk, T. Komolmis, and C. Ha Duyen (2007), Low latitude ionosphere-thermosphere dynamics studies with ionosonde chain in Southeast Asia, *Ann. Geophys.*, *25*, 1569–1577.

Nishida, A. (1968), Coherence of geomagnetic DP 2 fluctuations with interplanetary magnetic variations, *J. Geophys. Res.*, *73*, 5549–5559, doi:10.1029/JA073i017p05549.

Rastogi, R. G., and V. L. Patel (1975), Effect of interplanetary magnetic field on ionosphere over the magnetic equator, *Proc. Indian Acad. Sci.*, *82A*, 121.

Reddy, C. A., V. V. Somayajulu, and C. V. Devasia (1979), Global scale electrodynamic coupling of the auroral and equatorial dynamo regions, *J. Atmos. Sol. Terr. Phys.*, *41*, 189.

Santos, A. M., M. A. Abdu, J. H. A. Sobral, D. Koga, P. A. B. Nogueira, and C. M. N. Candido (2012), Strong longitudinal difference in ionospheric responses over Fortaleza (Brazil) and Jicamarca (Peru) during the January 2005 magnetic storm, dominated by northward IMF, *J. Geophys. Res.*, *117*, A08333, doi:10.1029/2012JA017604.

Senior, C., and M. Blanc (1984), On the control of magnetospheric convection by the spatial distribution of ionospheric conductivities, *J. Geophys. Res.*, *89*, 261–284, doi:10.1029/JA089iA01p00261.

Tsunoda, R. T., M. Yamamoto, T. Tsugawa, T. L. Hoang, S. Tulasi Ram, S. V. Thampi, H. D. Chau, and T. Nagatsuma (2011), On seeding, large-scale wave structure, equatorial spread F, and scintillations over Vietnam, *Geophys. Res. Lett.*, *38*, L20102, doi:10.1029/2011GL049173.

Tulasi Ram, S., P. V. S. Rama Rao, K. Niranjan, D. S. V. V. D. Prasad, R. Sridharan, C. V. Devasia, and S. Ravindhran (2006), The role of post sunset vertical drifts at the equator in predicting the onset of VHF scintillations during high and low sunspot activity years, *Ann. Geophys.*, *24*, 1609–1616.

Tulasi Ram, S., P. V. S. Rama Rao, D. S. V. V. D. Prasad, K. Niranjan, S. Gopi Krishna, R. Sridharan, and S. Ravindran (2008), Local time dependent response of post sunset ESF during geomagnetic storms, *J. Geophys. Res.*, *113*, A07310, doi:10.1029/2007JA012922.

Tulasi Ram, S., M. Yamamoto, R. T. Tsunoda, H. D. Chau, T. L. Hoang, B. Damtie, M. Wassaie, C. Y. Yatini, T. Manik, and T. Tsugawa (2014), Characteristics of large-scale wave structure observed from African and Southeast Asia longitudinal sectors, *J. Geophys. Res. Space Physics*, *119*, 1–10, doi:10.1002/2013JA019712.

Tulasi Ram, S., K. Sandeep, S.-Y. Su, B. Veenadhari, and S. Ravindran (2015), The influence of Corotating Interaction Region (CIR) driven geomagnetic storms on the development of equatorial plasma bubbles (EPBs) over wide range of longitudes, *Adv. Space Res.*, *55*, 535–544.

Yokoyama, T., R. F. Pfaff, M. Yamamoto, Y. Otsuka, M. Nishioka, and T. Tsugawa (2011), On postmidnight low-latitude ionospheric irregularities during solar minimum: 1. Equatorial Atmosphere Radar and GPS TEC observations in Indonesia, *J. Geophys. Res.*, *116*, A11325, doi:10.1029/2011JA016797.